Tomasz RYMARCZYK[1,2], Michał STYŁA[1], Michał OLESZEK[1], Michał MAJ[1,2], Konrad KANIA[3], Przemysław ADAMKIEWICZ[1,2]

Research & Development Centre Netrix S.A.(1), University of Economics and Innovation (2)

doi:10.15199/48.2020.01.40

Object detection using radio imaging tomography and tomographic sensors

***Abstract**. The article presents the method of detecting objects using radio tomography and tomographic sensors. The solution is based on measuring the radio signal strength between the transmitter and receiver. When measuring the object between the transmitter and the receiver, the value of the signal strength changes as a result of reflection, absorption or dispersion of electromagnetic waves. The application can determine the position using many Wi-Fi signal sources. The main task of the radio tomography presented in the work is to detect the presence of people in specific rooms in real time. As part of the research enabling image reconstruction, a transmission model was used. The measuring system consisted of sixteen antennas. The measured values were the received power expressed in dBm units in a straight line between the individual antennas.*

***Streszczenie.** Artykuł przedstawia metodę wykrywanie obiektów za pomocą tomografii radiowej i czujników tomograficznych. Rozwiązanie opiera się na pomiarze siły sygnału radiowego między nadajnikiem a odbiornikiem. W przypadku pomiaru obiektu między nadajnikiem a odbiornikiem wartość siły sygnału zmienia się w wyniku odbicia, absorpcji lub rozproszenia fal elektromagnetycznych. Aplikacja może określić pozycję za pomocą wielu źródeł sygnału Wi-Fi. Głównym zadaniem przedstawionej w pracy tomografii radiowej jest wykrywanie obecności ludzi w określonych pomieszczeniach w czasie rzeczywistym. W ramach badań umożliwiających rekonstrukcję obrazu zastosowano model transmisyjny. System pomiarowy składał się z szesnastu anten. Mierzone wartości były mocą odbieraną wyrażoną w jednostkach dBm w linii prostej między poszczególnymi antenami.. (**Wykrywanie obiektów za pomocą tomografii radiowej i czujników tomograficznych)**.*

Keywords: radio tomography imaging, sensors, image reconstruction.
Słowa kluczowe: tomografia radiowa, sensory, rekonstrukcja obrazu.

Introduction

The goal of the project and articles is to present a comprehensive device (device system) capable of measuring the strength of the received signal for the needs of a radio tomography and being able to act as a "Beacon" device. One of the main tasks of the system is the exchange of information between receivers and transmitters regarding the strength of the radio signal. After polling all devices, a measurement matrix will be created and the image reconstruction will be performed on its basis. The second main task of the system is to provide localization services using small radio transmitters called beacons [1-5]. There are many methods to solve optimization problems and being elements of a specific system [6-16]. In the tomography, deterministic methods and machine learning [17-36] are used to solve the inverse problem.

The development of electronics and computing methods, the IoT and the fall in prices of hardware equipment, has created favorable conditions for the development and expansion of existing intelligent building systems. At present, the potential of available technologies is not fully exploited and is usually limited to the ability to control devices using a tablet or smartphone. Technologies related to the accumulation and processing of large amounts of data and computational intelligence are not commonly used in building intelligent systems. The increasing availability of all types of sensors, falling electronic component prices, the growing popularity of Internet technology, and the potential of large data volumes generated by the building's use process, is a developing area that will be heavily exploited in the coming years. The proposed system enables one to adjust the beacon position using data from several receivers using tomographic techniques.

Real Time Locating Systems is one of the most dynamically developing branches of ICT. RLTS systems can be divided into systems operating in open spaces and working inside buildings. The first-class system primarily uses the Global Positioning System (GPS) technology in combination with cellular systems. Internal positioning systems cannot use GPS to determine indoor location. You can use Radio Tomography (RT) is a completely new technology for imaging objects with wireless networks or beacons. It offers a new way of displaying objects in buildings using the power of the received signal. The tomographic methods send signals along many different paths through the medium and measure the size and phase of the transmitted signal. Signals from a radio tomography can pass through obstacles such as walls, trees and smoke. It can work in the dark. Currently, in order to determine the approximate location of a mobile device, the index values of the radio signal strength (RSSI) between two devices covering the range of the same crossing operation are measured. Thanks to a hybrid model combining various interfaces and information from many sources. The system will be able to provide a more accurate position of the localized object.

Measurements

The main task of the presented device is to transmit, at a time interval, frames in the iBeacon standard via the Bluetooth module and to scan the environment in search of devices working in the same standard. When the device detects in its range the so-called Beacon, it automatically reads its identification data and signal strength and sends it via the MQTT protocol to the broker. Next, it is assumed that this data and data from other Beacons are properly analysed and processed into an image.

The test measurements were aimed at checking the operational parameters of currently used radio communication standards in terms of use in tomography. A measuring zone was established on the plan of a circle and a square with a diameter / side equal to 5 m. The zone was located in the possibly least vulnerable environment, i.e. in the underground garage, vulnerable to external electromagnetic fields. Measurements were carried out repeatedly - for different environmental conditions, for different sizes of system components (8 and 16 elements), for different positions and settings of measurement objects and radio modules and various measurement system configurations (eg: antennas, screens, type of modulation, signal strength).

Fig. 2. Measurement model.

In order to improve the reliability of the obtained results, isolate the system from the influence of external factors and guarantee the repeatability of measurements, all tested modules were equipped with copper screens that damped reflected waves. Based on the preliminary measurements it was possible to conclude that the presence of obstacles in the form of walls or large metal elements such as, for example, motor vehicles or trellis (Fig, 2) would negatively influence the measurement by inflating its value. Due to the transformation of the omnidirectional antenna into the directional antenna, an additional series of measurements was made to determine the dependence of the received signal strength depending on the angle of the transmitter and receiver position relative to each other. Summing up the performed tests.

Methods

The main task of the radio tomography presented in this work is to detect the presence of people in specific rooms in real time. This is possible thanks to the use of an 802.11 wireless network in the 2.4 gigahertz band - a microwave wave that belongs to the radio waves. Due to the absorption of microwave radiation through water, the phenomenon of dielectric losses, there is a noticeable loss of power in a given area. Physically it is connected with the orientation polarization, where the occurring chemical molecules (in this case water is a dipole) are positioned in the direction and the direction of the electric field of the electromagnetic wave acting on them.

As part of the research, enabling reconstruction of the image, a transmission model was used. The measuring system consisted of sixteen antennas. The measured values were the received power expressed in a unit of dBm in a straight line between individual antennas. The actual measurement was made on a circle with a radius of 2.5 m, the antenna was set at a height of 0.5 m, the antennas CC2543 were additionally shielded with copper. The measuring objects were a barrel with water and a man. Before placing the phantoms inside the study area, the background measurement was carried out - without the presence of objects. Measurements were made by measuring the power between each pair of antennas. Symmetry of measurements was assumed, this means that the measurement between two antennas is identical regardless of which of the antennas was the transmitting and receiving antenna. Therefore, the measurement sequence consisted in making measurements: between the first antenna and the antennas numbered from 2 to 16, then between the second and antennas numbered from 3 to 16 etc. The given sequence results in the execution $\binom{16}{2} = 120$ measurements in one measurement frame. In addition, it should be noted that the resolution has 32x32 pixels - so it is a vague system.

The next stage of the work was to design the matrix of the impact system. It was built using the Fresnel zone. The zone is an area that represents the shape of the radio signal energy transmission, its longitudinal cross section is an ellipse and the cross section is a circle. Propagation follows a straight line between the transmitter and the receiver, it should be noted that in the zone n = 1, the energy is the highest, then decreases after crossing the point P, where distances d1 and d2 are equal (Fig. 3). The shape of the rotational ellipsoid is variable and depends on the distance between the antennas and the radio frequency. The radius of the circle (r - expressed in meters), which the maximum value reaches in the middle of the distance between the antennas, can be calculated from the formula:

$$r = 8.657\sqrt{\frac{D}{f}},$$

where: D is the distance between the transmitting and receiving antennas and is expressed in meters, while f represents the frequency in gigahertz.

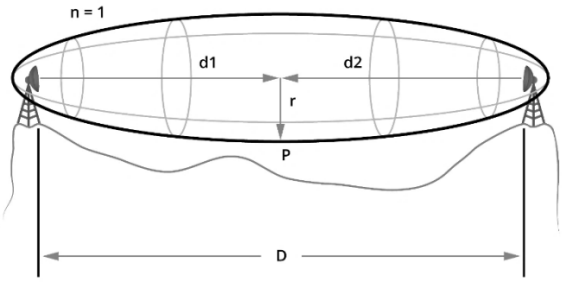

Fig. 3. Fresnel zone.

It is also worth adding that in creating the model, the filtering matrix in the form of Marra wavelet (also known as the Mexican Hat) was used. It is a spatial filter which is a second derivative of the normal distribution density and is expressed by the following formula:

$$mexHat(x,y) = \frac{1}{\pi\sigma^2}\left(1 - \frac{1}{2}\left(\frac{x^2+y^2}{\sigma^2}\right)\right)e^{-\frac{x^2+y^2}{2\sigma^2}}.$$

Its use has allowed to reduce the background noise. The deviation of the Marra wavelet used to build the model is equal to σ = 2.

Having a model and measurements, the reverse problem was solved, which were solved in two ways:

1. Using the singularity cut-off method (tSVD), with the cut-off threshold at th = 10.
2. Using regularization Tichonowa with a constant regularization parameter λ = 19000.

The algorithm begins its operation by calculating the vector of absolute differences between the actual measurement and the background measurement. Additionally, as part of the conducted research, in addition to the measured background, the background calculated from physical constants was used. Free-space path loss was used. It determines the decrease in the power of the electromagnetic wave signal as it moves along the line with the direct visibility of the antennas. On the other hand, free space determines that the phenomena of absorption, refraction, diffraction, reflection and scattering did not affect propagation. The FSPL can be calculated from the formula:

$$FSPl = 20 * log_{10}(D) + 20 * log_{10}(f) + 20 * log_{10}\left(\frac{4\Pi}{c}\right) - Gtx - Grx,$$

where: D is the distance between the antennas expressed in meters, f is the frequency in hertz, c is the speed of light in a vacuum, Gtx determines the gain of the transmitting antenna, while Grx the gain of the receiving antenna. Differences between the measured background and the calculated background can be seen in Fig. 4. It follows that the background image calculated from physical constants is not disturbed by the ambient conditions and the interference present in it. Therefore, assumptions have been made for the construction of the background matrix that result from the suppression assumed in the free space assumed by the phenomenon.

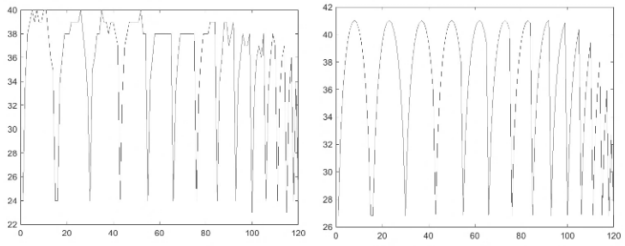

Fig. 4. Difference between the measured background and the calculated background.

Results

The next step in creating the algorithm was to determine the inverse matrix and calculate the image vector.
Algorithm:

- Calculation of the vector of absolute differences between the actual measurement and the background measurement
- Determining the inverse matrix and calculating the image vector
- The use of the Conventional Mexican Hat filter on the resulting image matrix
- Setting the image value (with a threshold of 50% of the maximum value)
- Visualization was made only within the field of view of the measuring system

The image reconstruction from results obtained using TI CC2543 are shown in Fig. 5 with one object in the position at 9 transmitter and with two objects in the position at 1 and 9 of the transmitters in Fig. 6.

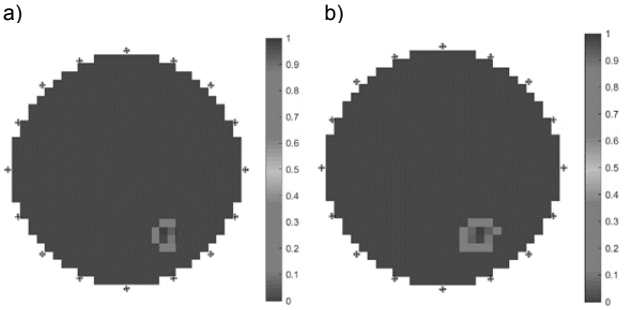

Fig. 5. Image reconstruction using beacons: a) SVD, b) Tikhonov.

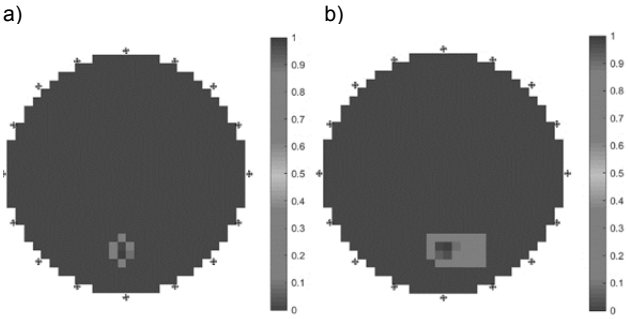

Fig. 6. Image reconstruction using TI CC2543: a) SVD, b) Tikhonov.

As you can see, the results differ only slightly depending on the adopted method. Both objects are clearly visible on the reconstructions and are located next to the appropriate antennas. Better mapping of the size, in particular the size of the barrel, occurs when using tSVD regularization. It is also worth adding that regardless of the choice of the background method, the results are almost identical. Unfortunately, in the reconstructed image, the objects are too close to the antennas in relation to their actual location.

In the case of regularization of Tikhonov, the shape of the phantoms and their location are much better. It should be noted that they are greatly enlarged in relation to their real size. In addition, for this method, the calculated background gives better results (Fig. 9 and 10).
The image reconstruction from results obtained using XBee are shown in Fig. 7 with one object in the position at 3 transmitter and with two objects in the position at 1 and 9 of the transmitters in Fig. 8.

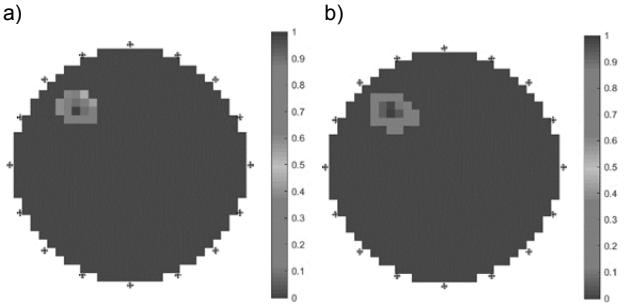

Fig. 7. Image reconstruction using XBee: a) SVD, b) Tikhonov.

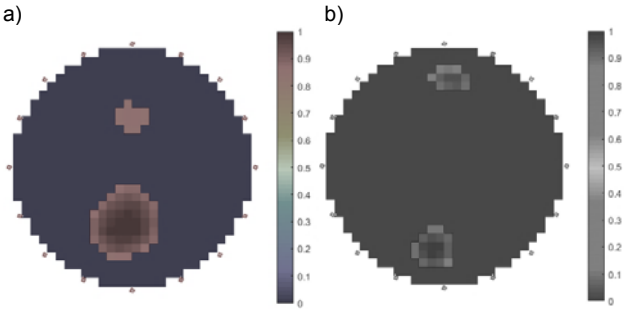

Fig. 8. Image reconstruction - background: a) regularization Tichonowa, b) regularization tSVD.

Conclusion

The article presents the development of a comprehensive system of devices capable of measuring the strength of the received signal for the needs of radio tomography One of the main tasks of the above The system is to exchange information between receivers and transmitters regarding the strength of the radio signal. After interrogating all devices, a measuring matrix is created and the image reconstruction based on it. The main task of radio tomography is to detect the presence of people in specific rooms in real time. This is possible thanks to the use of a wireless network. As part of the study, enabling image reconstruction, a transmission model was used. The measuring system consisted of sixteen antennas. The measured values were received power expressed in dBm units in a straight line between individual antennas. The analyzed objects are clearly visible on the reconstructions and are located next to the appropriate antennas. Better reproduction of the size, in particular the size of the barrel, occurs using tSVD regularization.

***Authors**: Tomasz Rymarczyk, Ph.D. Eng., University of Economics and Innovation, Projektowa 4, Lublin, Poland/ Research & Development Centre Netrix S.A. E-mail: tomasz@rymarczyk.com; Michal Styła, Research & Development Centre Netrix S.A. E-mail: michal.styla@netrix.com.pl; Michal Oleszek, Research & Development Centre Netrix S.A. E-mail: michal.oleszek@netrix.com.pl; Michał Maj, University of Economics and Innovation, Projektowa 4, Lublin, Poland/ Research & Development Centre Netrix S.A. E-mail: michal.maj@wse.lublin.pl; Przemysław Adamkiewicz, Ph.D., University of Economics and Innovation, Projektowa 4, Lublin, Poland/ Research & Development Centre Netrix S.A. E-mail: p.adamkiewicz@netrix.com.pl;*

REFERENCES

[1] Styla M., Oleszek M., Rymarczyk T., Maj M., Adamkiewicz P., Hybrid sensor for detection of objects using radio tomography, 2019 Applications of Electromagnetics in Modern Engineering and Medicine, PTZE 2019, 2019, 219-223

[2] Maj M., Rymarczyk T., Kania K., Niderla K., Styła M., Adamkiewicz P.: Application of the Fresnel zone and Free-space Path for image reconstruction in radio tomography, International Interdisciplinary PhD Workshop 2019, IIPhDW 2019, 15 – 17 May 2019, Wismar, Germany.

[3] Poole I., Free Space Path Loss: Details, Formula, Calculator, radio-electronics.com. Adrio Communications Ltd., Retrieved 17 July 2017

[4] Chełkowski A., Kluk E., Fizyka Dielektryków, Warszawa: Wydawnictwo Naukowe PWN, 1979.

[5] Dusiński A., Wybrane aspekty propagacji fal radiowych i zasady wymiarowania i projektowania systemów RST – materiały szkoleniowe dla MSWiA, 2005.

[6] Fiala P., Drexler P., Nešpor D., Szabó Z., Mikulka J., Polívka J., The Evaluation of Noise Spectroscopy Tests, ENTROPY, 18 (2016), No. 12, 1-16.

[7] Goetzke-Pala A., Hoła J., Influence of burnt clay brick salinity on moisture content evaluated by non-destructive electric methods. Archives of Civil and Mechanical Engineering, 16 (2016), No. 1, 101-111.

[8] Krawczyk A., Korzeniewska E., Łada-Tondyra E., Magnetophosphenes – History and contemporary implications, Przeglad Elektrotechniczny, 94 (2018), No 1, 61-64.

[9] Korzeniewska E., Szczesny A., Parasitic parameters of thin film structures created on flexible substrates in PVD process , Microelectronic Engineering, 193 (2018), 62-64.

[10] Lopato P., Herbko M., A Circular Microstrip Antenna Sensor for Direction Sensitive Strain Evaluation, Sensors, 18 (2018), No. 1, 310.

[11] Valis D., Mazurkiewicz D., Application of selected Levy processes for degradation modelling of long range mine belt using real-time data, Archives of Civil and Mechanical Engineering, 18 (2018), No. 4, 1430-1440.

[12] Valis D., Mazurkiewicz D., Forbelska M., Modelling of a Transport Belt Degradation Using State Space Model, Conference: IEEE International Conference on Industrial Engineering and Engineering Management (IEEE IEEM)Location: Singapore, Dec. 10-13, 2017, Book Series: International Conference on Industrial Engineering and Engineering Management IEEM, 2017, 949-953.

[13] Kozłowski E., Mazurkiewicz D., Żabiński T., Prucnal S., Sęp J., Assessment model of cutting tool condition for real-time supervision system, Eksploatacja i Niezawodnosc – Maintenance and Reliability, 21 (2019); No 4, 679–685

[14] Vališ D, Hasilová K., Forbelská M, Vintr Z, Reliability modelling and analysis of water distribution network based on backpropagation recursive processes with real field data, Measurement 149 (2020), 107026

[15] Kryszyn J., Smolik W., Toolbox for 3d modelling and image reconstruction in electrical capacitance tomography, Informatyka, Automatyka, Pomiary w Gospodarce i Ochronie Środowiska (IAPGOŚ) , 7 (2017), No. 1, 137-145

[16] Galazka-Czarnecka, I.; Korzeniewska E., Czarnecki A. et al., Evaluation of Quality of Eggs from Hens Kept in Caged and Free-Range Systems Using Traditional Methods and Ultra-Weak Luminescence, Applied Sciences-Basel, 9 (2019), No. 12, 2430.

[17] Babout L., Grudzień K., Wiącek J., Niedostatkiewicz M., Karpiński B., and Szkodo M., Selection of material for X-ray tomography analysis and DEM simulations: comparison between granular materials of biological and non-biological origins, Granul. Matter, 20 (2018), No. 3, 38.

[18] Banasiak R., Wajman R., Jaworski T., Fiderek P., Fidos H., Nowakowski J., Study on two-phase flow regime visualization and identification using 3D electrical capacitance tomography and fuzzy-logic classification, International Journal of Multiphase Flow, 58 (2014), 1-14.

[19] Grudzien K., Romanowski A., Chaniecki Z., Niedostatkiewicz M., Sankowski D., Description of the silo flow and bulk solid pulsation detection using ECT, Flow Measurement and Instrumentation, 21 (2010), No. 3, 198-206.

[20] Kryszyn J., Smolik W., Toolbox for 3d modelling and image reconstruction in electrical capacitance tomography, Informatyka, Automatyka, Pomiary w Gospodarce i Ochronie Środowiska (IAPGOŚ) , 7 (2017), No. 1, 137-145.

[21] Majchrowicz M., Kapusta P., Jackowska-Strumiłło L., Sankowski D., Acceleration of image reconstruction process in the electrical capacitance tomography 3d in heterogeneous, multi-gpu system, Informatyka, Automatyka, Pomiary w Gospodarce i Ochronie Środowiska (IAPGOŚ) , 7 (2017), No. 1, 37-41.

[22] Nowakowski J., Ostalczyk P., D. Sankowski, Application of fractional calculus for modelling of two-phase gas/liquid flow system, Informatyka, Automatyka, Pomiary w Gospodarce i Ochronie Środowiska (IAPGOŚ) , 7 (2017), No. 1, 42-45.

[23] Romanowski A., Big Data-Driven Contextual Processing Methods for Electrical Capacitance Tomography, in IEEE Transactions on Industrial Informatics, 15 (2019), No. 3, pp. 1609-1618.

[24] Romanowski A., Contextual Processing of Electrical Capacitance Tomography Measurement Data for Temporal Modeling of Pneumatic Conveying Process, 2018 Federated Conference on Computer Science and Information Systems (FedCSIS), IEEE, 2018, 283-286.

[25] Rymarczyk T, Kłosowski G. Innovative methods of neural reconstruction for tomographic images in maintenance of tank industrial reactors. Eksploatacja i Niezawodnosc – Maintenance and Reliability, 21 (2019); No. 2, 261–267

[26] Rymarczyk, T.; Kozłowski, E.; Kłosowski, G.; Niderla, K. Logistic Regression for Machine Learning in Process Tomography, Sensors, 19 (2019), 3400.

[27] Rymarczyk T., Szumowski K., Adamkiewicz P., Tchórzewski P., Sikora J., Moisture Wall Inspection Using Electrical Tomography Measurements, Przegląd Elektrotechniczny, 94 (2018), No 94, 97-100

[28] Duda K., Adamkiewicz P., Rymarczyk T., Niderla K., Nondestructive Method to Examine Brick Wall Dampness, International Interdisciplinary PhD Workshop Location: Brno, Czech Republic Date: SEP 12-15, 2016, 68-71

[29] Kłosowski G., Rymarczyk T., Gola A., Increasing the reliability of flood embankments with neural imaging method. Applied Sciences, 8 (2018), No. 9, 1457.

[30] Soleimani M., Mitchell CN, Banasiak R., Wajman R., Adler A., Four-dimensional electrical capacitance tomography imaging using experimental data, Progress In Electromagnetics Research, 90 (2009), 171-186.

[31] Smolik W., Kryszyn J., Olszewski T., Szabatin R., Methods of small capacitance measurement in electrical capacitance tomography, Informatyka, Automatyka, Pomiary w Gospodarce i Ochronie Środowiska (IAPGOŚ) , 7 (2017), No. 1, 105-110.

[32] Wajman R., Fiderek P., Fidos H., Sankowski D., Banasiak R., Metrological evaluation of a 3D electrical capacitance tomography measurement system for two-phase flow fraction determination, Measurement Science and Technology, 24 (2013), No. 6, 065302.

[33] M. Wang, Industrial Tomography: Systems and Applications, Elsevier, 2015.

[34] Ye Z., Banasiak R., Soleimani M., Planar array 3D electrical capacitance tomography, Insight: Non-Destructive Testing and Condition Monitoring, 55 (2013), No. 12, 675-680.

[35] Jiang Y., Soleimani M., Wang B., Contactless electrical impedance and ultrasonic tomography, correlation, comparison and complementary study, Measurement Science and Technology, 30 (2019), 114001

[36] Romanowski, A.; Łuczak, P.; Grudzień, K. X-ray Imaging Analysis of Silo Flow Parameters Based on Trace Particles Using Targeted Crowdsourcing, Sensors, 19 (2019), No. 15, 3317